IEEE Access
Multidisciplinary | Rapid Review | Open Access Journal

Received 21 November 2023, accepted 11 December 2023, date of publication 22 December 2023,
date of current version 4 January 2024.

Digital Object Identifier 10.1109/ACCESS.2023.3346062

RESEARCH ARTICLE

Construction of Dynamic Traffic Pattern Recognition and Prediction Model Based on Deep Learning in the Background of Intelligent Cities

JIAN CUI AND JIANYOU ZHAO
School of Automobile, Chang'an University, Xi'an 710064, China
Corresponding author: Jian Cui (cj15802963890@163.com)

ABSTRACT To reduce traffic congestion, it is particularly important to use advanced technology to predict urban traffic flow. Therefore, a dynamic traffic pattern prediction model is proposed, which includes convolutional neural network, long and short term memory network and attention mechanism. The validity of the prediction model is verified by the loss function and the average absolute percentage error. In addition, the study also constructs a model for user travel pattern and parking point recognition based on deep learning and mobile signaling data. The performance of the recognition model is verified by the accuracy and other indicators. The research outcomes demonstrated that the max average absolute percentage error of the dynamic traffic mode prediction model was 7.8%, and the mini value was 2.9%. The average accuracy of the user travel pattern recognition model was 83.34%, and that of the parking point recognition model was 88.56%.The dynamic traffic model recognition and prediction model designed by the research institute has better results, and has practical guiding significance in smart city traffic management.

INDEX TERMS Traffic mode, recognition, prediction, mobile signaling data, attention mechanism.

I. INTRODUCTION

With the acceleration of urbanization, the choice of residents' travel modes has also become an important concern factor in urban traffic governance [1], [2], [3]. The prediction of traditional transportation modes mostly uses Global Positioning System (GPS) data as the data source. Although results of this method are relatively rich, there are also issues with high acquisition costs and limited data coverage [4], [5], [6]. With the development of technology, the application value of mobile signaling data (MSD) and deep learning (DL) methods in traffic pattern recognition and prediction is gradually becoming prominent. However, these methods also have certain problems, such as not considering the impact of resident data on prediction results, having a relatively single influencing factor variable, and not considering the loss of sequence information caused by excessively long sequences [7], [8], [9]. Li et al. and other researchers proposed a new graph convolutional network model for accurate and real-time prediction of traffic flow. This model involved multiple sensor data, which can eliminate differences between periodic data and enhance the quality of input data [10]. Lin et al. and other experts designed a gradient-based regression tree method to study the dynamic spatiotemporal correlation of traffic flow, and used electronic registration recognition technology. This method could analyze the dynamic spatiotemporal correlation between prediction points and upstream correlation points, and accurately and timely predict rapidly changing traffic conditions [11]. Xiao et al. and other scholars designed a car following inertia gray model based on differential gray system information difference to predict short-term traffic flow. The prediction performance of this model on short-term traffic flow was superior to existing gray models [12]. However, these studies also have certain problems, such as less

The associate editor coordinating the review of this manuscript and approving it for publication was Emanuele Crisostomi.

TABLE 1. Formula abbreviation table.

K	Total number of trees	$l\left(y_i,\hat{y}^{(t)}\right)$	Loss function
i	The i-th vehicle	$\Omega\left(f_t\right)$	Regularization term
$\hat{y}_i$	Predicted value of i	A	The total number of leaf nodes
F	Set of all regression trees	γ 、 λ	Penalty coefficient
t	The t-th tree	j	The j-th leaf node
f_t	Functions represented by tree t	$cons$	The sum of the complexity of the first t-1 trees
$w_{q(x)}$	The weight of each leaf node	$\hat{y}^{(t-1)}$	The value of the t-1st tree of i
$q\left(x\right)$	Output the serial number of leaf nodes	g_i	First derivative of loss function
I_j	Sample set on leaf node with sequence number j	h_i	Second derivative of loss function
I_L	Sample group of left subtree	I_R	Sample group of right subtree
θ	The plane angle between the point on the connecting sphere and the center radius R of the sphere	$harversin$	Haversine formula
$\alpha^i_{e\_lat}$	Starting latitude of base station	$\alpha^i_{s\_lat}$	End the latitude of the base station
d	Distance between base stations	$\alpha^i_{e\_lng}$	Start the longitude of the base station
$\alpha^i_{s\_lng}$	End the longitude of the base station	ς	Space distance between base stations
$T^i_{s\_time}$	Start time of data	$T^i_{e\_time}$	End time of data
Θ	Road non linear coefficient	A^i_a	User's acceleration
S^i_v	Average speed of users	T_i	User's travel time

TABLE 1. *(Continued.)* Formula abbreviation table.

D_i	User's travel distance	S	Standard deviation
X	Calculate samples	$\overline{X}$	Average
SSE	Clustering error of samples	C_i	Cluster
p	Sample points of clusters	m_i	The centroid of a cluster
x	Absolute value of acceleration	μ	Shape parameter
z	Position parameters	U_j	Joint membership value
s_j	Average speed membership value	a_j	Acceleration membership value
U_i	Travel mode labels corresponding to the maximum membership value	s	Travel distance based on mobile signaling trajectory data
d_j	Similarity value between mobile signaling trajectory data and navigation data	TM	Time threshold
R_j	Maximum similarity value between navigation data and mobile signaling trajectory data	φ	Input variables

consideration of pre-identification of user stopping points, significant errors in link trajectories, and failure to consider the impact of multiple factors on traffic flow. Based on these problems, the research innovatively proposed a dynamic traffic pattern recognition and prediction (DTPRP) model combining convolutional neural network (CNN), long and short-term memory network (LSTM) and attention mechanism (AM), and established parking point recognition (PPR) model and user travel mode recognition model based on MSD and eXtreme Gradient Boosting (XGBoost) algorithm. The first part of the study introduces the relevant research on DTPRP, and the second part constructs a DL-based DTPRP model. The third part of the study analyzes the recognition and prediction results of the model, while the fourth part presents the conclusions and shortcomings of the study.

There are three main contributions to the research. Firstly, the research aims to analyze the dynamic traffic patterns of smart cities, identify different user travel modes, and analyze the impact of combined features on user travel modes. Secondly, the research aims to provide technical and information support for urban traffic management and guidance in

smart cities based on the analysis of dynamic traffic patterns, enhance the scientific and rational nature of intelligent urban traffic management, promote the prosperity and development of urban traffic, and establish a traffic governance system. Thirdly, the research aims to alleviate traffic congestion in smart cities through scientific and reasonable urban traffic management, improve user travel efficiency, and reduce user congestion time on the road.

There are two innovative points in the research. The first is the use of XGBoost algorithm and K-means clustering algorithm in identifying user travel patterns. The second is the integration of CNNs, LSTMs, and AMs in the construction of DTPRP models. The study uses a large number of formulas, and for the convenience of querying, a table of formula abbreviations is created, as shown in Table 1.

II. RELATED WORKS

With the increasing severity of random traffic congestion and the advancement of science and technology, more researchers have conducted research on the DTPRP. To avoid the shortcomings of traditional methods for traffic arrival patterns, researchers such as C. An proposed a method to estimate lane-based traffic arrival patterns with license plate recognition data. This method used a probability model and assumed the upstream merging motion as a two-stage segmented arrival process. The research results showed that this method could describe traffic arrival models under different traffic scenarios [13]. To detect outlier in traffic flow (TF), Wang et al. and other scholars proposed an efficient traffic anomaly detection framework. The framework used the non negative matrix decomposition algorithm to pre-process the data, used the fuzzy C-means clustering algorithm with the optimal K-cluster center to extract the road TF patterns, and used kernel density estimation to fit the probability density of the road TF matrix. The laboratory findings expressed that the mean accuracy and recall of this method were 95% and 96.%, respectively [14]. To better detect unauthorized wireless cameras, experts such as Cheng et al. proposed a lightweight and effective detection mechanism based on smartphones and a human assisted recognition model, which utilized the inherent traffic patterns of wireless camera traffic. The research findings illustrated that the model's accuracy was as high as 98% [15]. Ramkumar et al. and other researchers have proposed an advanced driving assistance system to better ensure the safety of humans while driving vehicles. This system could effectively recognize road signs and transmit information to drivers in a timely manner. The experimental results showed that the system could classify more than 40 types of traffic signs with high accuracy [16]. He et al. and other scholars put forward a new semi supervised learning method to utilize a small amount of labeled traffic sign data to establish an efficient and high-quality traffic sign recognition model. This method combined global and local features of traffic sign recognition on transportation systems based on the Internet of Things. It was validated that this method's effectiveness was superior to that of traditional methods [17]. To reduce the error of estimating annual average daily traffic from sample data, experts such as G. Grande proposed a method to quantify the error range, and used a new data-driven allocation method to lessen the error, which could reduce the average absolute error by 2.46% [18].

Liu et al. and other researchers proposed a pattern recognition method based on image processing to reduce the incidence of highway traffic accidents. This method used the fuzzy C-means clustering algorithm in the clustering algorithm, and used the Relief and particle swarm optimization algorithms to optimize it. The research findings indicated that the optimized algorithm had better real-time performance and accuracy [19]. Xiao et al. and other experts put forward a hybrid model that combined integrated empirical mode decomposition, deep belief networks, and Google Trends to accurately predict tourism transportation demand. This model used integrated empirical mode decomposition to de-noise the data. The laboratory findings denoted that the model had lower prediction error and higher prediction accuracy [20]. Sun et al. such as Sun put forward a multi-component attention model to predict TF. The model involved one-dimensional CNNs and bidirectional LSTM. It was proved that compared with artificial neural networks, the proposed model had good accuracy and effectiveness in predicting urban TF [21]. Shi et al. proposed an end-to-end attention-based periodic time neural network to predict traffic. This network simulated spatial and periodic dependencies through an encoder AM. The research findings expressed that the proposed model could better capture dependencies and avoid over-fitting of nodes [22]. Sun et al. such as Du raised a dynamic transfer CNN to improve the effectiveness of traffic demand prediction. This network could be used for precise prediction of traffic demand. The experimental results demonstrated that this method had good performance in predicting traffic demand [23]. Chen et al. and other experts proposed a DL based framework for forecasting urban road TF. This framework used feature engineering for feature extraction. The laboratory outcomes denoted that the average prediction accuracy of this method was close to 98% [24].

In summary, there are currently many studies on DTPRP, and the methods involved are also diverse. However, these studies also have certain problems, such as the relatively single influencing factor variable and the failure to consider the loss of sequence information caused by excessively long sequences. Based on these problems, the research innovatively proposed a DTPRP model combining CNN, LSTM and AM, and established PPR model and user travel mode recognition model based on MSD and XGBoost algorithm. There are other strategies and methods that can improve the prediction results of TF parameters. Firstly, it needs to select input data, that is, select and filter data from the input model to improve data quality. This not only improves the prediction accuracy of the model, accelerates the training speed of the model, but also reduces the risk of over-fitting in the model. Secondly, it also needs to improve the generalization performance of the model, select appropriate optimization

TABLE 2. Detailed information on literature review.

Number	Objective	Solution	Result
[13]	Avoiding the shortcomings of traditional methods	Identifying data/Probability models through license plates	This method can describe the traffic arrival modes of upstream merged TFs under different traffic scenarios, and is more reliable than the baseline method
[14]	Detecting outliers in TF	Traffic anomaly detection framework/ K-clustering center, C-means clustering algorithm	The average values of accuracy and recall are 95.38% and 96.23% respectively, and the average detection time is 28.4 seconds
[15]	Update of detection methods	Lightweight and effective detection mechanism and human assisted recognition model based on smartphones	Detect the camera with an accuracy of over 97% within 2 to 7 seconds
[16]	Ensuring driving safety	Advanced assistance system/License plate recognition	The recognition accuracy is as high as 95.78%, and the average recognition time is 185ms
[17]	Establish a traffic sign recognition model	A new semi-supervisedlearning method	This method is superior to existing baseline methods, with a recognition accuracy of up to 99%
[18]	Reduce errors in annual average daily traffic volume	Quantification error range	The average absolute errors of counting and data-driven allocation methods are 6.40% and 7.86%, respectively
[19]	Reduce the probability of traffic accidents	Pattern recognition method based on image processing/ Fuzzy C-means clustering, Relief algorithm, and particle swarm optimization algorithm	This improved algorithm has good real-time performance and accuracy in parallel pattern recognition of urban expressways
[20]	Predict tourism transportation demand	A Hybrid model integrating empirical mode decomposition, deep belief network, and google Trends	The prediction error of the model is significantly lower than the baseline of the deep belief network, resulting in higher prediction accuracy
[21]	Predicted TF	Multicomponent attention model/One dimensional convolutional network and bidirectional long short term memory	It can meet the accuracy and effectiveness requirements of complex nonlinear urban TF prediction models.
[22]	Predicting Traffic	End-to-end attention based periodic time neural network	Capable of capturing spatial and periodic dependencies, with advanced predictive performance
[23]	Enhance traffic prediction performance	Dynamic transfer CNN	Experiments were conducted on shared data of taxis and bicycles, demonstrating the good performance of the prediction model
[24]	Predicting TF	A framework for predicting urban road TFbased on DL	The average prediction accuracy is close to 97.7%
This paper	Identify and predict dynamic traffic patterns	A dynamic traffic pattern prediction model that integrates	The average accuracy of the user travel mode and PPR model is 83.34% and 88.56%,

TABLE 2. *(Continued.)* **Detailed information on literature review.**

	CNN, LSTM, and AM, combining user travel patterns and PPR models	respectively. The maximum accuracy of the dynamic traffic mode prediction model is 99.4%

methods, and perform multi model fusion. Thirdly, it needs to avoid gradient disappearance or explosion. Fourthly, the parameters of the model should be moderate and not too large. The detailed information of the literature review is shown in Table 2.

III. CONSTRUCTION OF DTPRP MODEL BASED ON DL

To identify and predict dynamic traffic patterns and alleviate urban congestion, different DL algorithms are used to identify users' parking points and travel patterns using MSD as the entry point, and their respective recognition models are established. In addition, the study combines DL methods such as MSD and CNNs to generate a DTPRP model.

A. DESIGN OF USER TRAVEL PATTERNS RECOGNITIONBASED ON DL

Resident travel information is an important basis for urban transportation planning, so it is necessary to identify and analyze user travel patterns, and stopping point recognition is an important foundation for analyzing user travel patterns [25], [26]. Traffic mode refers to the methods or means of transportation used by residents for travel. Therefore, by identifying users' travel modes and stopping points, it is possible to understand the commonly used means of transportation by residents, which is also an important component of dynamic traffic mode prediction. The current dynamic traffic pattern prediction model has certain shortcomings in identifying user travel patterns, as it does not consider the impact of combined features on user travel patterns [27]. Before identifying and designing user travel patterns, to reduce prediction errors, the XGBoost algorithm is introduced in the study. This algorithm belongs to the classification regression algorithm and can fit the previous tree's residual by continuously iterating to generate a new tree [28], [29]. The tree model of XGBoost algorithm adopts a classification regression tree, and uses the weighted values of K trees as the prediction results of the sample. The prediction function is shown in equation (1).

$$\begin{cases} \widehat{y}_i = \sum_{t=1}^{k} f_t(x_i),\ f_t \in F \\ f_t(x) = w_{q(x)} \end{cases} \tag{1}$$

In equation (1), i is the ith vehicle. $\widehat{y}_i$ means the predicted value of i. F denotes the set of all regression trees. f_t is the expression expressed by the tree t. $w_{q(x)}$ indicates the weight of every leaf node, and $q(x)$ expresses the serial amount of the output leaf node. The objective expression of the XGBoost algorithm is shown in equation (2).

$$\begin{cases} Obj^{(t)} = \sum_{i=1}^{t} l\left(y_i, \widehat{y}^{(t)}\right) + \sum_{i=1}^{t} \Omega(f_t) \\ \Omega(f_t) = \gamma A + \frac{1}{2}\lambda \sum_{j=1}^{A} w_j^2 \end{cases} \tag{2}$$

In equation (2), $l\left(y_i, \widehat{y}^{(t)}\right)$ means the loss function. $\Omega(f_t)$ indicates the regularization term. A denotes the total number of leaf nodes. γ and λ are the penalty coefficient, and j refers to the j_{th} leaf node. Taking the total of the complexity of the previous $t-1$ trees as a constant, equation (3) can be obtained.

$$Obj^{(t)} = \sum_{i=1}^{n} l\left(y_i, \widehat{y}^{(t-1)} + f_t(x_i)\right) + \Omega(f_t) + cons \tag{3}$$

In equation (3), $cons$ is the sum of the complexity of the previous $t-1$ trees, and $\widehat{y}^{(t-1)}$ denotes the value of the $t-1$ tree of i. By solving the mini value of the objective function at $f_t = 0$ using Taylor's quadratic expansion, the objective function is approximated as equation (4).

$$\begin{cases} Obj^{(t)} \approx \sum_{i=1}^{n} l\left(y_i, \widehat{y}^{(t-1)} + g_i f_t(x_i) + \frac{1}{2} h_i f_t^2(x_i)\right) \\ +\Omega(f_t) + cons \\ g_i = \partial_{\widehat{y}^{(t-1)}} l\left(y_i, \widehat{y}^{(t-1)}\right) \\ h_i = \partial^2_{\widehat{y}^{(t-1)}} l\left(y_i, \widehat{y}^{(t-1)}\right) \end{cases} \tag{4}$$

In equation (4), $l\left(y_i, \widehat{y}^{(t-1)}\right)$ means the loss function of the learning model formed by the previous $t-1$ decision tree, and g_i, h_i are the first and the second derivative of the loss function of the model respectively. Substituting equation (2) into equation (4) yields equation (5).

$$Obj^{(t)} = \sum_{j}^{A} \left[G_j w_j + \frac{1}{2}\left(H_j + \lambda\right) w_j^2 \right] + \gamma A \tag{5}$$

In equation (5), $G_j = \sum_{i \in I_j} g_i$, $H_j = \sum_{i \in I_j} h_i$, $I_j = \{i | q(x_i) = j\}$ refer to the sample set on the leaf node with sequence number j. After taking the derivative of w_j in equation (2), equation (6) can be obtained.

$$w_j^* = -\frac{G_j}{H_j + \lambda} \tag{6}$$

After substituting the optimal solution of equation (6) into equation (5), the mini objective function of the XGBoost model can be obtained, as shown in equation (7).

$$obj = -\frac{1}{2} \sum_{j=1}^{A} \frac{G_j}{H_j + \lambda} + \gamma A \tag{7}$$

Due to the fact that the structure of the tree cannot be fully enumerated, the XGBoost algorithm needs to use greedy algorithms to partition the sub-trees of the current node.

When adding or listing segmentation points, it is generally recommended to select the partition with the smallest objective function and the most significant gain. The gain expression is shown in equation (8) [30].

$$Gain = -\frac{1}{2}\left[\frac{G_L^2}{H_L+\lambda}+\frac{G_R^2}{H_R+\lambda}-\frac{G_L+G_R}{H_R+\lambda}\right]-\gamma \quad (8)$$

In equation (8), $G_L = \sum_{i\in I_L} g_i$, $G_R = \sum_{i\in I_R} g_i$, $H_L = \sum_{i\in I_L} h_i$, $H_R = \sum_{i\in I_R} h_i$, I_L and I_R mean the sample groups of the left and right sub-trees, respectively. For user travel patterns recognition, the research mainly utilizes the XGBoost model. The algorithm framework for user travel patterns recognition is shown in Figure 1.

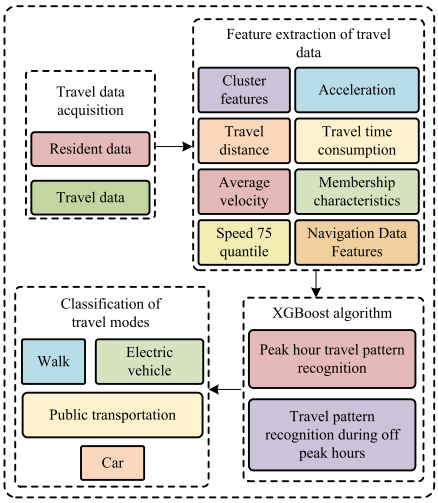

FIGURE 1. User travel patterns recognitionframework.

In Figure 1, the user travel patterns recognition is mainly composed of four stages, namely travel data acquisition and special effects extraction, XGBoost algorithm construction, and travel pattern classification. In the stage of obtaining travel data, signaling data can be divided into travel and dwell data through the identification of dwell points. In the feature extraction stage of travel data, the study extracts multidimensional spatiotemporal features such as average speed and acceleration, navigation data, clustering and membership features, and fuses them with peak and off peak periods to establish a multi-dimensional spatiotemporal optimal feature matrix. In the construction phase of XGBoost algorithm, a multi-dimensional spatiotemporal optimal feature matrix is added to complete the design of a user travel patterns recognition model. Finally, in the travel mode classification stage, the XGBoost algorithm outputs four user travel modes. For the extraction of average velocity and acceleration features, the Euclidean distance between base stations is calculated, and the calculation expression is shown in equation (9).

$$\begin{cases} harver\sin(\theta) = \dfrac{1-\cos\theta}{2} \\ \varsigma = \cos\left(\alpha_{e\_lat}^i\right)\times\cos\left(\alpha_{s\_lat}^i\right) \\ \times harver\sin\left(\dfrac{\alpha_{e\_\ln g}^i-\alpha_{s\_\ln g}^i}{2}\right) \\ +harver\sin\left(\alpha_{e\_lat}^i-\alpha_{s\_lat}^i\right) \\ d = 2\times R\times\arcsin\left(\sqrt{\varsigma}\right) \end{cases} \quad (9)$$

In equation (9), *harver* sin means the haversine equation, and θ stands for the plane angle between the point connecting the sphere and the radius R of the sphere center. $\alpha_{e\_lat}^i$ and $\alpha_{s\_lat}^i$ represent the latitude of the starting and ending base stations in the i_{th} data. d means the distance between base stations. $\alpha_{e\_\ln g}^i$ and $\alpha_{s\_\ln g}^i$ express the longitude of the starting and ending base stations in the i_{th} data, and ς denotes the spatial distance between base stations. The duration calculation of MSD is shown in equation (10)

$$T = T_{e\_time}^i - T_{s\_time}^i \quad (10)$$

In equation (10), $T_{s\_time}^i$ refers to the start time of the i_{th} data, and $T_{e\_time}^i$ indicates the end time of the i_{th} data. The average speed and acceleration of MSD are calculated as shown in equation (11).

$$\begin{cases} D = 2\times d_i\times\Theta \\ S_v^i = \dfrac{D_i}{T_i} \\ A_a^i = \dfrac{\left|S_v^{i+1}-S_v^i\right|}{T_i} \end{cases} \quad (11)$$

In equation (11), Θ is the non-linear coefficient of the road, and the default value is 1.3. A_a^i represents the acceleration of the i_{th} data user, and A_a^i stands for the average speed of the i_{th} data user. T_i means the travel time of the user in data i, and D_i indicates the travel distance of the user in data i. For the extraction of clustering features, the k-means clustering algorithm is used in the study [31]. To normalize traffic data, the Z-score method [32] is used in the study, and its calculation is shown in equation (12).

$$Z = \frac{X-\overline{X}}{S} \quad (12)$$

In equation (12), S expresses the standard deviation. X refers to a certain sample, and $\overline{X}$ stands for the average of this set of data. To get better clustering results, the optimal number of clusters K value for k-means clustering is determined using the elbow method [33]. The calculation of the sum of squares of the core indicator error of this method is shown in equation (13).

$$SSE = \sum_{i=1}^{k}\sum_{p\in C_i}\left|p-m_i\right|^2 \quad (13)$$

In equation (13), *SSE* means the clustering error of all samples. C_i stands for the i_{th} cluster. p indicates the sample point

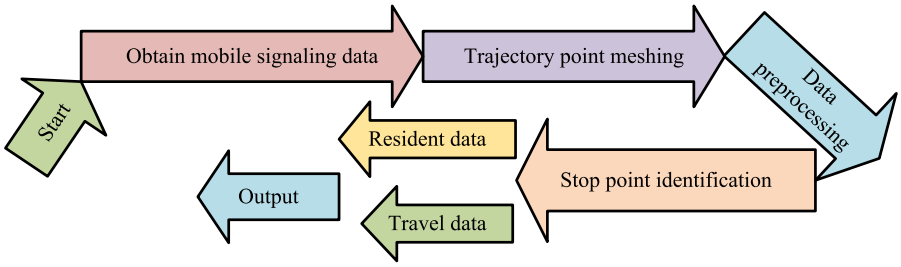

FIGURE 2. Flow chart of stop point recognition model.

of C_i, and m_i denotes the centroid of C_i, which is the mean of all samples in C_i. The expression of the Gaussian membership is shown in equation (14).

$$g(x, \mu, z) = e^{\left(\frac{(x-z)^2}{2\mu^2}\right)} \tag{14}$$

In equation (14), x indicates the absolute value of average velocity or acceleration, while μ and z are represented as shape parameters and position parameters, respectively. By using the Gaussian membership function, the membership values corresponding to average velocity and acceleration can be obtained, and their calculation is shown in equation (15).

$$U_j = s_j \times a_j \, (j = 1, 2, 3, 4) \tag{15}$$

In equation (15), U_j expresses the joint membership value of travel mode j. s_j means the average speed membership value of travel mode j, and a_j denotes the acceleration membership value of travel mode j. The calculation of the travel mode label corresponding to the maximum membership value is shown in equation (16).

$$U_i = MAX\left(U_j\right) (j = 1, 2, 3, 4) \tag{16}$$

In equation (16), U_i is the travel mode label corresponding to the maximum membership value of the i_{th} data. The extraction of navigation data features is mainly achieved by calculating the similarity between MSD and corresponding navigation data, as shown in equation (17).

$$\begin{cases} d_j = \dfrac{1}{\sqrt{\left(s - s_j\right)^2 + \left(t - t_j\right)^2}} \, (j = 1, 2, 3, 4) \\ R_j = MAX\left(d_j\right) (j = 1, 2, 3, 4) \end{cases} \tag{17}$$

In equation (17), d_j means the similarity value between the mobile signaling trajectory data and the j_{th} navigation data, and R_j indicates the maximum similarity value between the j navigation data and the mobile signaling trajectory data. s denotes the travel distance of the mobile signaling trajectory data, and t refers to the travel time consumption of the mobile signaling trajectory data. s_j stands to the travel distance of type j navigation data, and t_j denotes the travel time consumption of type j navigation data. By extracting different features and using the XGBoost algorithm, the user travel patterns recognition during peak and off peak hours is studied and achieved.

B. DESIGN OF STOP POINT RECOGNITION AND CONSTRUCTION OF DTPRP MODEL BASED ON MSD

PPR is the foundation of user travel mode analysis, and to alleviate urban traffic congestion, research has designed it. However, the current dynamic traffic mode prediction models also have certain shortcomings in identifying stopping points, as they do not consider the impact of stopping data on the prediction results [34], [35]. A spatiotemporal grid clustering algorithm for PPR has been proposed. This algorithm performs feature analysis on MSD in both temporal and spatial dimensions, and uses PPR algorithm to identify parking points. This algorithm is not affected by the unstable sampling interval of signaling data, and its PPR model flowchart is shown in Figure 2.

In Figure 2, the PPR model mainly includes four parts, namely obtaining MSD, trajectory point meshing, data preprocessing, and PPR. The identification of parking points mainly falls into two situations: parking data and travel data.Based on the positioning function of mobile phone signaling data, trajectory point meshing can map the user's trajectory points in the grid and store them in the signaling database. Data preparation mainly involves processing error data in mobile phone signaling data. The recognition of stopping points is mainly achieved through a time-space grid clustering stopping point recognition algorithm.The collection of MSD is shown in Figure 3.

As shown in Figure 3, the collection of MSD is mainly divided into three layers: the collection layer, the sharing layer, and the application layer. At collection layer, data from different network scenarios will be collected and transmitted to the shared layer.The signaling data involved in the collection layer includes mobile phone signaling data under the second, third, fourth, and fifth generation mobile communication technologies. Among them, the second generation mobile communication technology will go through processes such as signaling gateways and aggregation and diversion, while the third, fourth, and fifth generation mobile communication technology will go through deep detection of traffic aggregation adapters, aggregation and diversion, and data packets.The MSD under the second-generation mobile communication technology will enter the signaling monitoring of the shared layer after being processed by the client/server protocol and analyzed by Gb/Iu-Ps collection. The MSD under

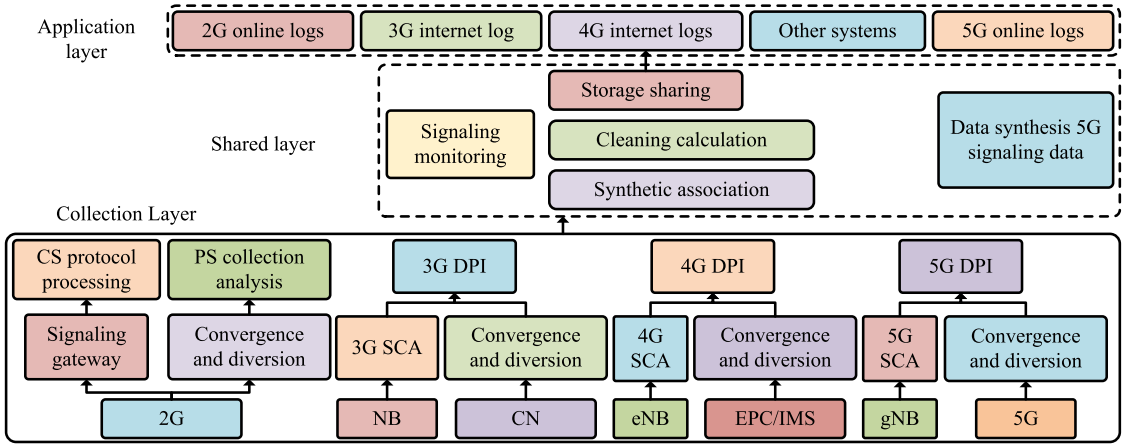

FIGURE 3. The collection of MSD.

the third, fourth, and fifth generation mobile communication technologies will be transmitted to the shared layer after Deep Packet Inspection (DPI). DPI is a network security technology that checks the content of network packets to determine their purpose and source, ensuring network security. In the sharing layer, data from the 5th generation (5G) mobile communication technology scenario will be synthesized into 5G signaling data and 5G internet logs will be generated on subsequent application layers. The data in other scenarios will go through three steps under the shared layer, namely synthesis association, cleaning calculation, and storage sharing. Subsequently, these data will generate corresponding online logs at the application layer. In addition, to protect user privacy, the signaling collection system will anonymously process MSD before uploading it to the cloud server. The specific steps of meshing trajectory points are generally composed of three steps. First is to treat the location of the base station as the center of the grid and the coverage of the base station as edge length of the grid. The second step is to map the trajectory points to the grid of the studied traffic area through their latitude and longitude position information. The third step is to store the trajectory data and its corresponding grid data together in the signaling database.

The error data in MSD can generally be divided into two categories: intrinsic error and systematic error [36]. There are four main types of system errors, namely table tennis switching, missing, repeated positioning and drift data [37]. For inherent errors, it is currently difficult to completely correct them in offline state and can only be approximated as much as possible. For missing data, i.e. data with both longitude and latitude of 0, it needs to simply remove it. For duplicate positioning data, it merges them using a rule-based approach. For table tennis switching data, a filtered table tennis switching data algorithm is used in the study. This algorithm utilizes grid processing methods and the feature of data quickly jumping between adjacent base stations, and sets the time threshold TM. For drift data, the study uses a filtered drift data algorithm. For the parking points recognition, after the spatiotemporal grid clustering, PPR algorithm gridizes the traffic area, calculates the continuous dwell time of users in each grid and sets the time threshold. If the continuous residence time of a user in a certain grid is less than the time threshold TM, then the data in that grid is the travel trajectory data, otherwise it is the residence trajectory data. TF prediction is also an important component of dynamic traffic mode prediction [38]. TF refers to the number of vehicles in the road network, so predicting TF is the prediction of the number of vehicles in the road network. Traffic mode refers to the methods or means of transportation used by residents for travel. By predicting TF, the situation of residents using vehicles for travel can be understood. The current dynamic traffic mode prediction model still has certain shortcomings, as it also considers less about the spatiotemporal properties and external environment of TF [39].In the construction of DTPRP model, CNN, LSTM and AM in the DL method are all applied. The main function of the CNN model is to collect features from data, and it mainly includes convolutional, activated, pooling and fully connected layers [40], [41]. Common activation function of CNN models include Sigmoid [42], ReLU [43] and tanh functions [44], and their calculations are shown in equation (18).

$$\begin{cases} Sigmoid\ (\varphi) = \dfrac{1}{1+e^{-\varphi}} \\ \tanh\ (\varphi) = \dfrac{e^{\varphi}-e^{-\varphi}}{e^{\varphi}+e^{-\varphi}} \\ \mathrm{Re}LU\ (\varphi) = \max\ (0, \varphi) \end{cases} \tag{18}$$

Equation (18), φ is the input variable. LSTM network is a variant of recurrent neural network (RNN), which has the features of long term memory [45], [46]. The temporal features of dynamic traffic mode TF data can be extracted using LSTM networks, while spatial features can be extracted using CNN networks. Based on the collected spatiotemporal features, the matrix of TF data can be constructed. Through inputting the spatiotemporal characteristics of TF into the regression prediction layer, the corresponding prediction results can be calculated. AM is a type of DL theory that can improve the predictive ability of models [47], [48]. The

construction of a DTPRP model mainly includes two steps. First is to pre-process the data, and the second is to build a prediction model. Data pre-processing includes four stages: PPR, dataset partitioning and time feature transformation, user travel patterns recognition, and data standardization. In the stage of PPR, different error data have different data processing methods. The data with latitude and longitude of 0 are directly removed, and the overlapping data are merged using rule-based methods. The ping-pong switching data and drift data are filtered through a grid spatiotemporal connection algorithm. Finally, the parking points are identified using the spatiotemporal grid clustering PPR algorithm. The recognition of travel models is mainly achieved by inputting the XGBoost model with the optimal feature matrix of multi-dimensional spatiotemporal trajectories. Dataset partitioning and temporal feature transformation include converting the MSD into a TF dataset, and partitioning the dataset with a 5-minute time interval. There are 288 samples generated every day, and each sample has a corresponding label. Data standardization can eliminate the impact of dimensional and value range differences among various styles of data. By using the minimum maximum normalization method, the values of the raw data are mapped to the range [0,1]. Traffic flow prediction (TFP) includes short and long-term ones, and the former is the key to alleviating traffic congestion [49], [50]. The short-term TFP model based on AM and CNN-LSTM is shown in Figure 4.

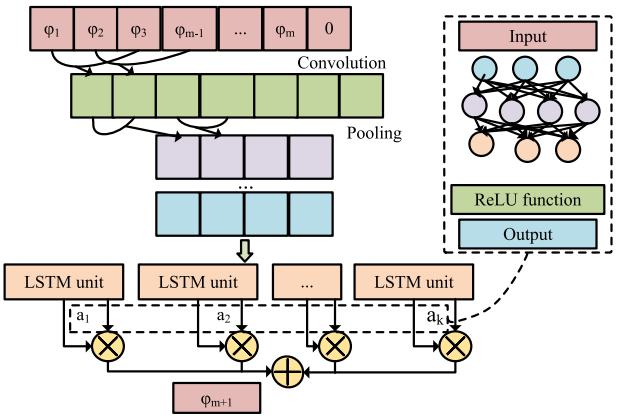

FIGURE 4. A short-term TFP model based on AM and CNN-LSTM.

As shown in Figure 4, the short-term TFP contains CNN, LSTM, and AMs. The prediction steps of this model generally include five steps. The first is to first get road TF and weather data, and then pre-process these data to construct the matrix dataset. The dataset contains training and testing sets. The second is to extract the spatial features of TF data with a CNN network. The third is to use the spatial features extracted from the CNN model as input to the LSTM network and output the temporal features of TF. The fourth is to dynamically fit the weight distribution through the AM, giving more weight to important features. The fifth step is to input spatiotemporal features into the regression prediction layer and calculate the corresponding prediction outcomes. In addition, by defining the loss function, the model parameters are continuously optimized.

IV. ANALYSIS OF THE RESULTS OF DTPRP MODEL CONSTRUCTION BASED ON DL

To evidence the performance of the PPR algorithm, this chapter selected four indicators: accuracy, recall, precision, and F1 value. In addition, this chapter also analyzed the data pre-processing results of the PPR algorithm. To verify the performance of user travel recognition algorithms, this chapter compared and analyzed the accuracy of features of various travel modes in the XGBoost model, and also compared the recall and accuracy of different models in signaling data. In addition, this chapter also evaluated the prediction accuracy of DTPRP models using absolute percentage error (APE) [51].

A. ANALYSIS OF PPR AND USER TRAVELPATTERNS RECOGNITION RESULTS BASED ON MSD

The data pre-processing stage of the PPR algorithm involved a variety of error data types, among which the most typical error data was ping-pong switching data. In data pre-processing, if the value of the time threshold *TM* was too small, it would lead to incomplete data filtering during ping pong switching. The filtering effect of ping-pong switching data for different users under different time thresholds is shown in Figure 5.

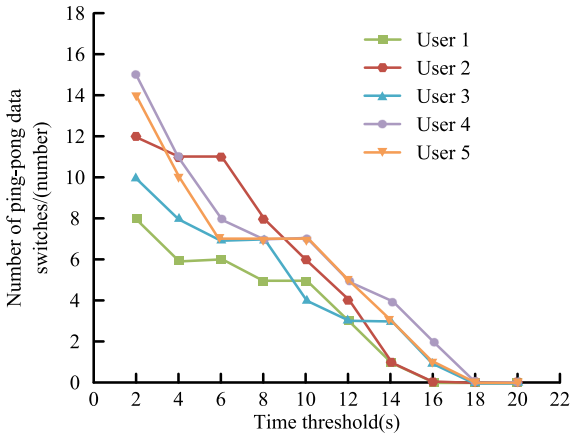

FIGURE 5. The filtering effect of Ping-pong switching data for different users under different time thresholds.

From Figure 5, the maximum number of ping-pong switching data for the five users was 15, 14, 12, 10, and 8, respectively, and these maximum values corresponded to a time threshold of 2 seconds. The minimum number of ping-pong switching data for five users was 0, and the time threshold at this time was 18 seconds. From this, when the time threshold was 18s, the filtering effect of ping pong switching data was the best. To ensure the scientific nature of the time threshold, the study increased the number of users. In addition, to reduce unnecessary losses, the initial value

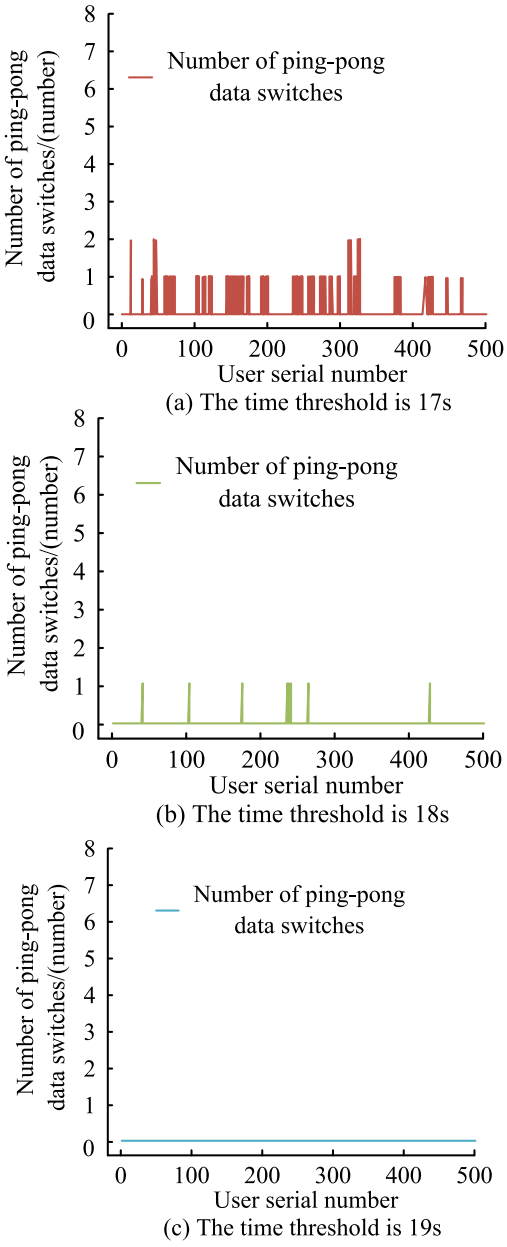

FIGURE 6. The filtering effect of Ping-pong switching data for different users at a time threshold of 17s to 19s.

of the time threshold was set to 17 seconds. The filtering effect of ping-pong switching data for different users at a time threshold of 17s to 19s is shown in Figure 6.

From Figure 6 (a), when the time threshold was 17s, the maximum number of ping-pong switching data was 2 and the minimum value was 0. The number of ping-pong switching data with 0 and 1 was roughly the same. In Figure 6 (b), if the time threshold was 18s, the biggest value of the number of ping-pong switching data was 1 and the minimum value was 0. There were more ping-pong switching data with 0 than ping-pong switching data with 1. From Figure 6 (c), when the time threshold was 19s, the biggest and lowest values of the amount of ping pong switching data were both 0, and that for all users was 0. When the time threshold was 19s, the filtering

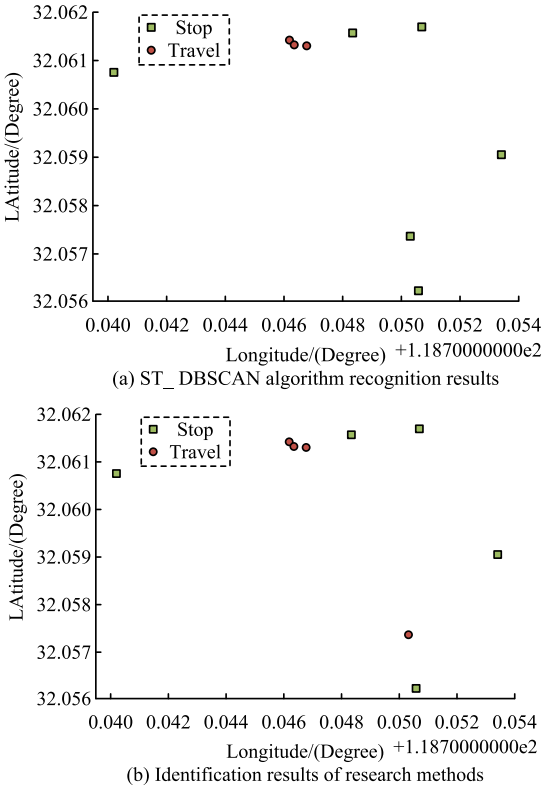

FIGURE 7. Comparison of stop point recognition results.

effect of ping-pong switching data was the best. To better reflect the effectiveness of the PPR algorithm proposed by the research institute, ST was selected for the study. The ST_DBSCAN algorithm [52] was used to compare the PPR results with the PPR algorithm proposed in the research. The specific comparison results are shown in Figure 7.

As shown in Figure 7 (a), the ST_DBSCAN algorithm identified 3 parking points and 6 travel points. From Figure 7 (b), the PPR algorithm proposed by the research institute identified 4 parking points and 5 travel points. Due to the fact that there were four actual parking points, the PPR algorithm proposed by the research institute had better performance in PPR. To evidence the performance of the PPR algorithm proposed by the research institute, the study compared and analyzed it and ST_DBSCAN algorithm from four perspectives: recall rate, F1 value, accuracy, and precision. The algorithms' comparison outcomes are expressed in Figure 8.

From Figure 8 (a), the biggest accuracy, recall rate, F1 value and precision of the PPR algorithm proposed by the research institute were89.4%, 85.2%, 83.5%, and 82.1%, respectively.The lowest valueswere 87.8%, 83.7%, 81.6%, and 80.2%, respectively.The average valueswere 88.56%, 84.82%, 82.72%, and 80.9%, respectively. From Figure 8 (b), the biggest accuracy recall rate, F1 value and precision of the ST_DBSCAN algorithm were 86.5%, 78.9%, 78.2%, and 78.2%, respectively.The lowest valueswere 84.6%, 77.8%, 76.5%, and 76.4%, respectively.The average valueswere

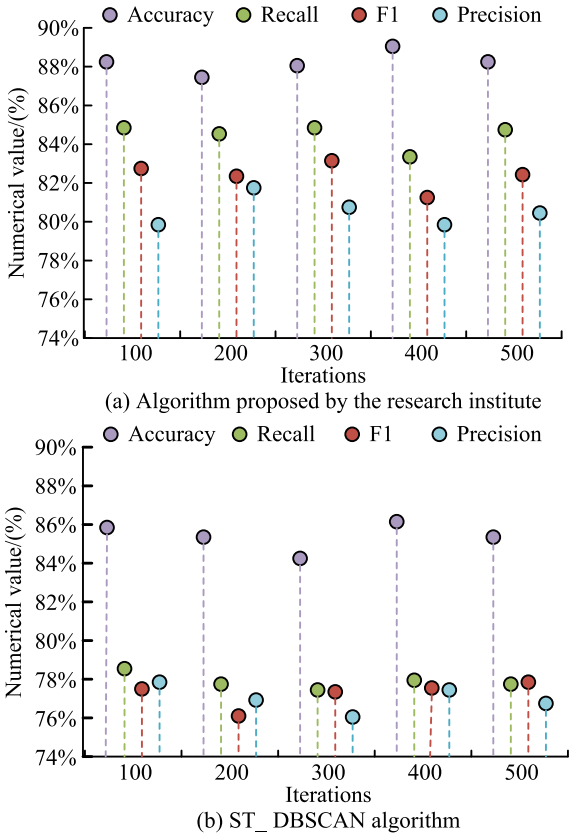

FIGURE 8. Algorithm performance comparison results.

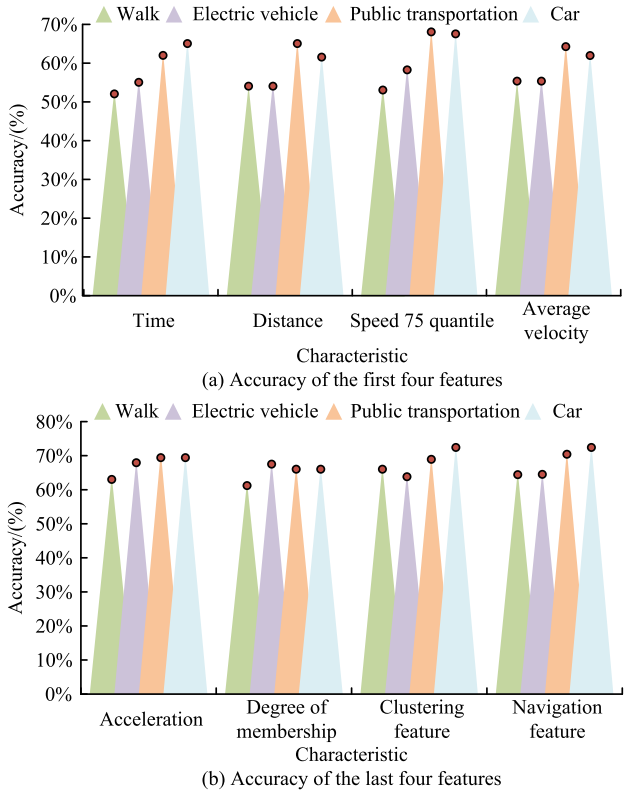

FIGURE 9. Accuracy of different travel modes with different features in XGBoost model.

85.74%, 78.24%, 77.63%, and 77.36%, respectively. From this, the PPR algorithm proposed by the research institute performed better than ST_DBSCAN algorithm in accuracy, recall, F1 value, and precision. To verify the effectiveness of user travel data features, the study inputted all eight features of user travel data into the XGBoost model. The accuracy of different travel modes with different features in the XGBoost model is shown in Figure 9.

From Figure 9 (a), the biggest value of time feature accuracy was 55.5% for cars, the lowest value was 53% for walking, and the average value was 54.18%. The biggest value of distance feature accuracy was 59.2% for public transportation, the lowest value was 55% for electric vehicles, and the average value was 56.63%. The biggest value of speed 75 quantile feature accuracy rate was 69% of public transport, the lowest value was 63% of walking, and the average value was 65.8%. The biggest accuracy of average speed characteristics was 68.5% for public transportation, the lowest was 62.5% for electric vehicles, and the average was 65.03%. From Figure 9 (b), the biggest value of acceleration feature accuracy was 67.1% for public transportation, the lowest value was 62.3% for electric vehicles, and the average value was 64.75%. The biggest accuracy of membership feature was 69% for walking, the lowest was 64.9% for public transportation, and the average was 67.03%. The biggest accuracy of clustering features was 71.5% for small cars, 67.1% for electric cars, and the average was 69.95%. The biggest value of navigation feature accuracy was 74% for small cars, the lowest value was 67.1% for electric cars, and the average value was 71.28%. From this, all 8 features of user travel data were valid features. To prove the function of the XGBoost model, some classic machine learning models were selected for comparison. The selected comparison models included multi-layer perceptron (MLP) model [53], K-Nearest Neighbor (KNN) model [54], Decision Tree (DT) model [55], Random Forest (RF) model [56] and Back Propagation (BP) model [57]. The comparison results of recall and precision of different models are shown in Figure 10.

From Figure 10 (a), the max recall rate of the MLP, KNN, DT, RF, BP and XGBoost models was 78.5%, 79%, 80.5%, 80.7%, 81.9% and 82.3%, respectively. The mini values were 76.7%, 77.4%, 76.6%, 79%, 80.6%, and 80.7%, respectively. The average values were 77.5%, 78.08%, 79.04%, 81.04%, and 81.62%, respectively. In Figure 10 (b), the max precision of the MLP, KNN, DT, RF, BP and XGBoost models was 76%, 77.2%, 77%, 77.6%, 81.3%, and 81.2%, respectively. The mini values were 74.8%,75.8%, 76.1%, 77.1%, 78.5%, and 80%, respectively. The average values were75.42%, 76.34%, 77.26%, 79.68%, and 80.5%, respectively. The comparison results of F1 values and accuracy of different models are shown in Figure 11.

From Figure 11 (a), the max F1 value of the MLP,KNN, DT, RF, BP and XGBoost models was 76.5%, 77.8%, 78.7%,

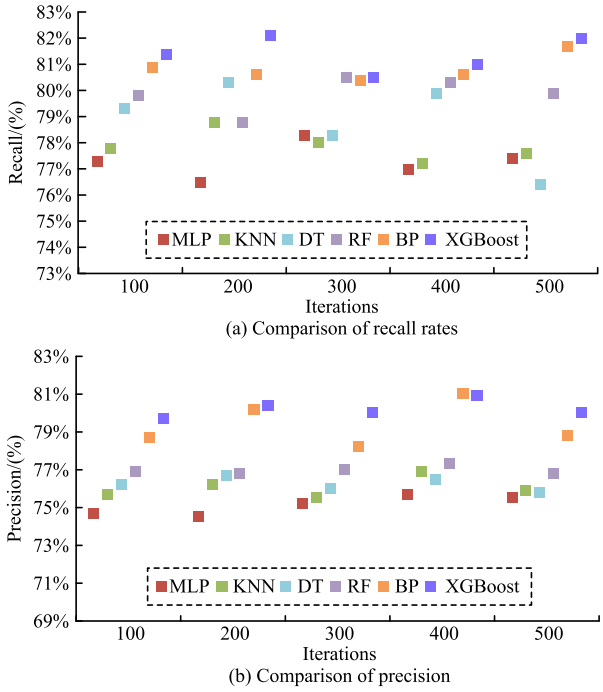

FIGURE 10. Comparison results of recall and precision of different models.

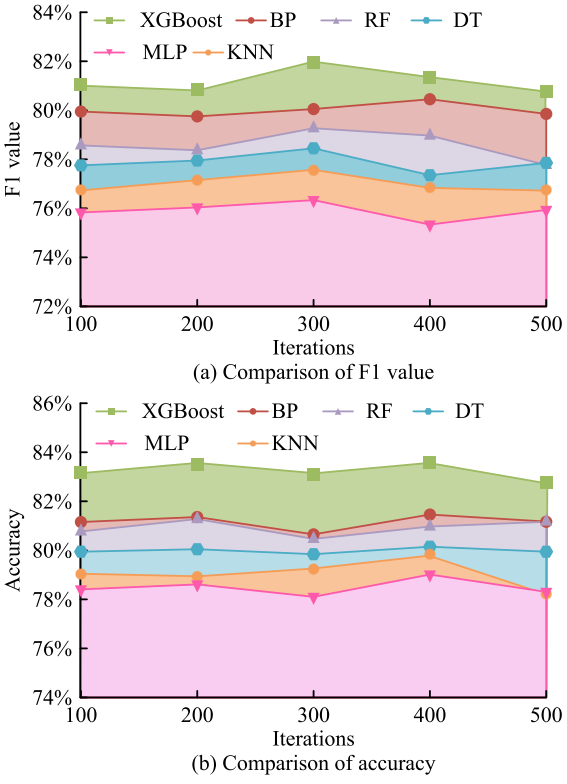

FIGURE 11. Comparison results of F1 values and accuracy among different models.

79.6%, 80.7%, and 82.2%, respectively. The mini values were 75.5%, 77%, 77.6%, 78.1%, 80%, and 81%, respectively. The average values were 76.06%, 77.26%, 78.12%, 78.92%, 80.26%, and 81.44%, respectively. From Figure 11 (b), the max accuracy of the MLP, KNN, DT, RF, BP and XGBoost models was 79.1%, 80%, 80.3%, 81.5%, 81.6%, and 83.7%, respectively. The mini values were 78.2%, 78.4%, 80%, 80.7%, 80.8%, and 82.9%, respectively. The average values were 78.58%, 79.22%, 80.14%, 81.16%, 81.3%, and 83.34%, respectively. From this, the performance of the XGBoost model was superior to that of the comparative model. To evaluate the impact of multidimensional features on the accuracy of user travel patterns recognition, the importance of sample features was ranked in the study. In addition, to verify the impact of peak and off peak periods on prediction results, the accuracy of the optimal combination of multidimensional spatiotemporal features at different time periods was compared and analyzed. The importance results of sample features and the prediction results at different time periods are displayed in Figure 12.

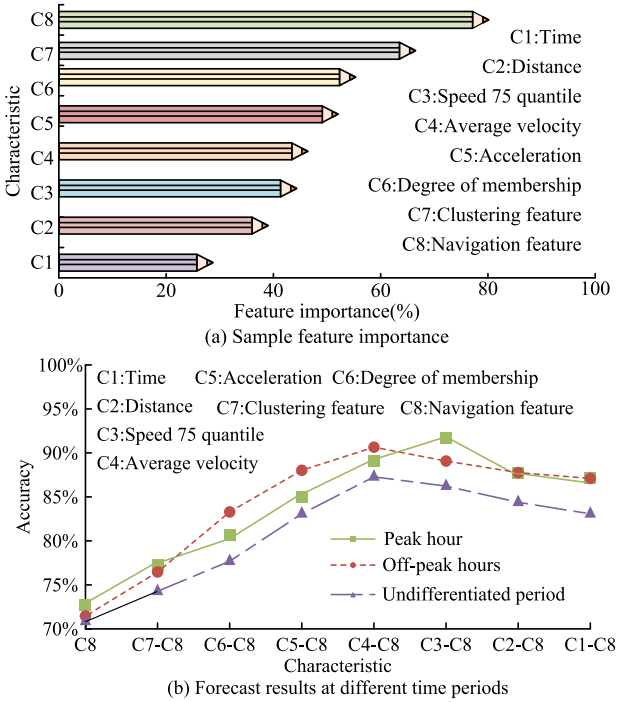

FIGURE 12. Sample feature importance results and prediction results at different time periods.

From Figure 12 (a), the maximum value of feature importance was 72% of the navigation feature, and the minimum value was 26% of the time feature. Navigation features had the greatest impact on the accuracy of user travel recognition. As shown in Figure 12 (b), the maximum accuracy during peak hours was 92%, while the minimum accuracy was 72.5%. The maximum accuracy during off peak hours was 90.5%, and the minimum accuracy was 71%. The maximum and minimum accuracy values for undifferentiated time periods were 87% and 70.3%, respectively. From this, the XGBoost model had a prediction accuracy of over 90% during peak and off peak periods.

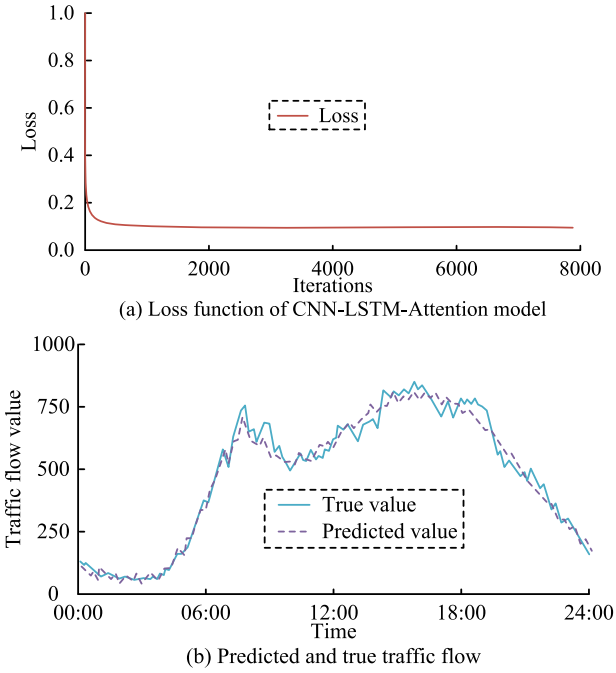

FIGURE 13. The loss function of the CNN-LSTM attention model and the predicted and true values of TF.

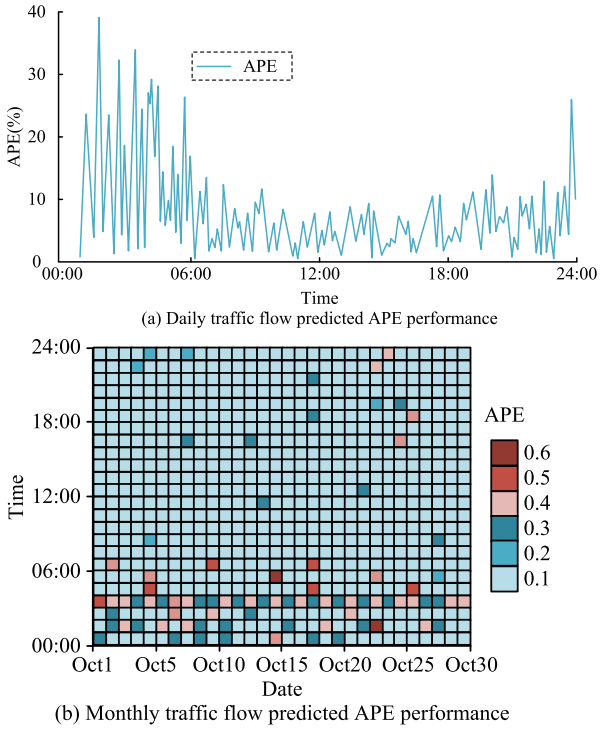

FIGURE 14. APE performance analysis of daily TFP and monthly TFP.

B. ANALYSIS OF THE RESULTS OF CONSTRUCTING A DTPRP MODEL BASED ON DL

To validate the function of the CNN-LSTM Attention model, the study trained and evaluated the model, and did comparison and analysis of predicted and true values, and APE values of TF. The operating system used in the experiment was Windows 10, and MSD from a certain section of Tianfu Third Street in Chengdu provided by a mobile operator was selected, and the converted data capacity was KB. In addition, Python was used for coding experiments, as well as the Keras framework and Baidu Map application programming interface tool library. The loss function of the CNN-LSTM Attention model and the predicted and true values of TF are shown in Figure 13.

From Figure 13 (a), at the beginning of the iteration, the loss function value of the CNN-LSTM Attention model showed a rapid decline trend. After the loss function continued to iterate several times, the model's loss function value presented a gentle trend and gradually realized convergence. From Figure 13 (b), the max predicted value was 800 and the mini value was 49. The max value of the true value was 850, and the mini value was 51. The distinguish between the predicted and the actual values was not significant, and there was a basically consistent trend of change. The APE performance analysis for daily TF and monthly TFP is expressed in Figure 14.

APE can evaluate the predictive accuracy of the model. From Figure 14 (a), within the time range of a day, the maximum value of APE was 39%, appearing around 1am, and the minimum value was 0%. It occurred at multiple time points, such as 0am, 5:40am, and 9pm.The values with higher APE values were mainly distributed between the early morning and 6 am, while the values with lower APE were mainly distributed between 6 am and before the early morning. As the time approached 12pm, there was a significant increase in APE values. From Figure 14 (b), the distribution of the max APE value was mainly concentrated between early morning and 6 am, especially between 4am and 5am, over a period of one month, while APE values were relatively small at other times, especially between 8am and 4pm. From this, the CNN-LSTM Attention model had good feasibility and effectiveness. To verify the feasibility of adding weather condition input variables and further evaluate the effectiveness of the CNN-LSTM Attention model, the study compared and analyzed the average APE function of the model under different environments, and also compared and analyzed the MAPE values of different prediction models. The comparison outcomes are shown in Figure 15.

Figure 15 (a) depicts the comparison of the average APE between the CNN-LSTM Attention model with and without weather factors, with a sampling frequency of 5 minutes. Figure 15 (b) shows the average APE comparison of different prediction models. From Figure 15 (a), under the same sampling interval, the max average APE value of the CNN LSTM Attention model with and without considering weather factors was 7.8% and 8%, respectively. and the mini values were 4% and 2.8%, respectively. From this, the prediction error of the CNN-LSTM Attention model considering weather factors was smaller. From Figure 15 (b), the max average APE value of the CNN-LSTM Attention, CNN, LSTM and CNN-LSTM models was respectively 7.8%, 12%, 10.75% and 8.1%. And

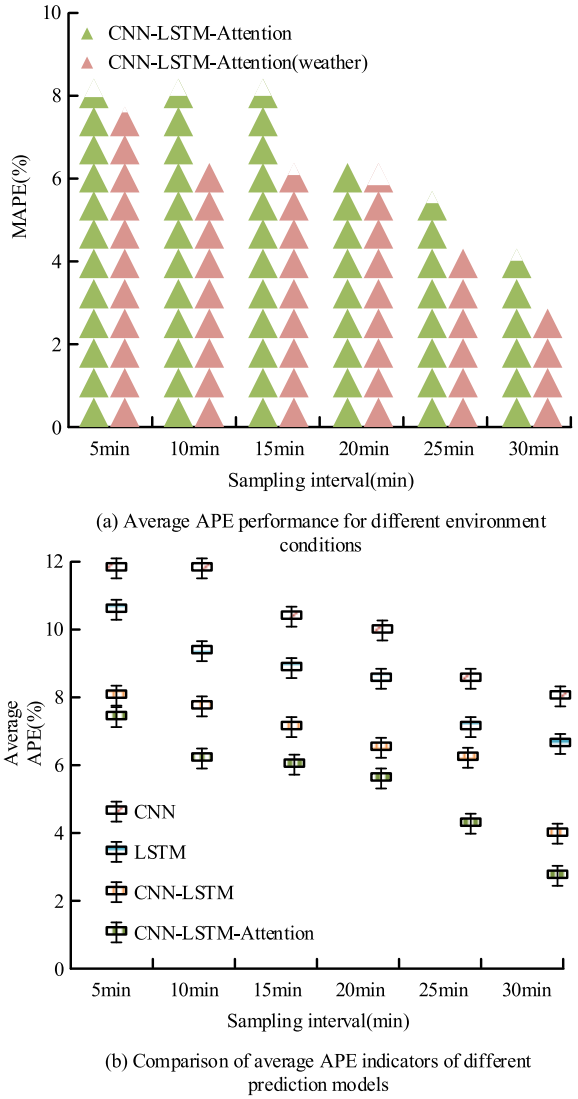

(a) Average APE performance for different environment conditions

(b) Comparison of average APE indicators of different prediction models

FIGURE 15. Comparison of average APE values under different environments and prediction models.

the mini values were 2.9%, 8.2%, 6.9% and 4%. From this, the CNN-LSTM Attention model had smaller prediction errors and better prediction performance. To better reflect the performance of the dynamic traffic mode prediction model designed by the research institute, the accuracy of the model predictions was compared. The comparison models include CNN, LSTM, CNN-LSTM, Auto-regressive Integrated Moving Average (ARIMA) model and ARIMA-LSTM model of LSTM [58], SARIMA-AR model combining seasonal difference Auto-regressive moving average (SARIMA) model and Auto-regressive (AR) model [59], GRU-CNN-Attention model combining Gated Recurrent Unit (GRU), CNN and AM [60].

In Table 3, the maximum prediction accuracy of the CNN-LSTM Attention model was 99.4%, and the minimum value was 98.6%. The maximum prediction accuracy of the CNN model was 91.8%, and the minimum value was 89.6%.

TABLE 3. Comparison of accuracy between different models.

Model	Number of experiments			
	1	2	3	4
CNN	89.6%	90.1%	91.8%	89.9%
LSTM	91.2%	92.4%	93.6%	92.8%
CNN-LSTM	94.3%	93.2%	95.5%	93.8%
CNN-LSTM-Attention	98.6%	99.4%	98.9%	99.1%
ARIMA-LSTM	95.8%	96.5%	96.9%	97.2%
SARIMA-AR	96.3%	97.6%	97.9%	96.8%
GRU-CNN-Attention	95.1%	96.6%	97.4%	97.7%

The maximum prediction accuracy of the LSTM model was 93.6%, and the minimum value was 91.2%. The maximum prediction accuracy of the CNN-LSTM model was 95.5%, and the minimum value was 93.2%. The maximum prediction accuracy of the ARIMA-LSTM model was 97.2%, and the minimum value was 95.8%. The maximum prediction accuracy of the SARIMA-AR model was 97.9%, and the minimum value was 96.3%. The maximum prediction accuracy of the GRU-CNN Attention model was 97.7%, and the minimum value was 95.1%. The accuracy of the CNN-LSTM Attention model was higher than that of the comparative model, which also indicated that the performance of the model was better.

V. CONCLUSION

To address the issue of urban road congestion in the environment, a DTPRP model combining CNN, LSTM, and AM has been innovatively proposed. A PPR model and a user travel patterns recognition model have been established based on MSD and XGBoost algorithm. The research outcomes expressed that the average accuracy, recall, F1 value, and precision of the PPR model used by the research institute were 88.56%, 84.82%, 82.72%, and 80.9%, respectively, which were 2.82%, 6.58%, 5.09%, and 3.54% higher than the average accuracy, recall, F1 value, and precision of the comparison algorithm. From this, the effectiveness and superiority of the PPR algorithm used by the research institute could be validated. The accuracy and average F1 value of the user travel patterns recognition model based on XGBoost algorithm used by the research institute were 83.34% and 81.44%, respectively, and both were higher than the accuracy and average F1 value of the comparative model. The max and mini average APE values of the CNN-LSTM-Attention model used by the research institute were 7.8% and 2.9%, respectively, and the average APE values of the comparative model were generally higher than those of the CNN-LSTM-Attention model. From this, the model used by the research institute had smaller prediction errors and better prediction performance. Although various influencing factors have been considered in the identification and DTPRP models, there are also certain shortcomings, such as the generalization of signaling user trajectories and the lack of fine-grained stop point recognition for signaling users, which can be promoted in future research.

REFERENCES

[1] C. Lin, G. Han, J. Du, T. Xu, L. Shu, and Z. Lv, "Spatiotemporal congestion-aware path planning toward intelligent transportation systems in software-defined smart city IoT," *IEEE Internet Things J.*, vol. 7, no. 9, pp. 8012–8024, Sep. 2020.

[2] J. Jin, D. Rong, Y. Pang, F. Zhu, H. Guo, X. Ma, and F.-Y. Wang, "PRECOM: A parallel recommendation engine for control, operations, and management on congested urban traffic networks," *IEEE Trans. Intell. Transp. Syst.*, vol. 23, no. 7, pp. 7332–7342, Jul. 2022.

[3] T. Wang, R. Cheng, and H. Ge, "Analysis of an extended two-lane lattice hydrodynamic model considering mixed traffic flow and self-stabilization effect," *Eng. Comput.*, vol. 38, no. 1, pp. 58–82, Jun. 2020.

[4] Z. Xiao, X. Fu, L. Zhang, and R. S. M. Goh, "Traffic pattern mining and forecasting technologies in maritime traffic service networks: A comprehensive survey," *IEEE Trans. Intell. Transp. Syst.*, vol. 21, no. 5, pp. 1796–1825, May 2020.

[5] C. Xu, C. Xu, and T. Truong, "Mining the spatio-temporal pattern using matrix factorisation: A case study of traffic flow," *IET Intell. Transp. Syst.*, vol. 14, no. 10, pp. 1328–1337, Oct. 2020.

[6] Q. Huang, Y. Yang, Y. Xu, F. Yang, Z. Yuan, and Y. Sun, "Citywide road-network traffic monitoring using large-scale mobile signaling data," *Neurocomputing*, vol. 444, pp. 136–146, Jul. 2021.

[7] J. Li, J. Li, N. Jia, X. Li, W. Ma, and S. Shi, "GeoTraPredict: A machine learning system of Web spatio-temporal traffic flow," *Neurocomputing*, vol. 428, pp. 317–324, Mar. 2021.

[8] M. Bhanu, J. Mendes-Moreira, and J. Chandra, "Embedding traffic network characteristics using tensor for improved traffic prediction," *IEEE Trans. Intell. Transp. Syst.*, vol. 22, no. 6, pp. 3359–3371, Jun. 2021.

[9] D. Ma, X. Song, and P. Li, "Daily traffic flow forecasting through a contextual convolutional recurrent neural network modeling inter- and intra-day traffic patterns," *IEEE Trans. Intell. Transp. Syst.*, vol. 22, no. 5, pp. 2627–2636, May 2021.

[10] W. Li, X. Wang, Y. Zhang, and Q. Wu, "Traffic flow prediction over mutisensor data correlation with graph convolution network," *Neurocomputing*, vol. 427, pp. 50–63, Feb. 2021.

[11] L. Zheng, J. Yang, L. Chen, D. Sun, and W. Liu, "Dynamic spatial–temporal feature optimization with ERI big data for short-term traffic flow prediction," *Neurocomputing*, vol. 412, pp. 339–350, Oct. 2020.

[12] X. Xiao, H. Duan, and J. Wen, "A novel car-following inertia gray model and its application in forecasting short-term traffic flow," *Appl. Math. Model.*, vol. 87, pp. 546–570, Nov. 2020.

[13] C. An, X. Guo, R. Hong, Z. Lu, and J. Xia, "Lane-based traffic arrival pattern estimation using license plate recognition data," *IEEE Intell. Transp. Syst. Mag.*, vol. 14, no. 4, pp. 133–144, Jul. 2022.

[14] X. Wang, R. Zeng, F. Zou, F. Huang, and B. Jin, "A highly efficient framework for outlier detection in urban traffic flow," *IET Intell. Transp. Syst.*, vol. 15, no. 12, pp. 1494–1507, Dec. 2021.

[15] Y. Cheng, X. Ji, T. Lu, and W. Xu, "On detecting hidden wireless cameras: A traffic pattern-based approach," *IEEE Trans. Mobile Comput.*, vol. 19, no. 4, pp. 907–921, Apr. 2020.

[16] S. Ramkumar, K. Sridhar, and R. Ganapathy, "Traffic sign detection and recognition using CNN," *ECS Trans.*, vol. 107, no. 1, pp. 17447–17455, Apr. 2022.

[17] Z. He, F. Nan, X. Li, S. Lee, and Y. Yang, "Traffic sign recognition by combining global and local features based on semi-supervised classification," *IET Intell. Transp. Syst.*, vol. 14, no. 5, pp. 323–330, May 2020.

[18] G. Grande, P. Paramita, and J. D. Regehr, "Data-driven approach to quantify and reduce error associated with assigning short duration counts to traffic pattern groups," *Transp. Res. Record, J. Transp. Res. Board*, vol. 2675, no. 9, pp. 271–283, Mar. 2021.

[19] Z. Liu, H. Jia, and Y. Wang, "Urban expressway parallel pattern recognition based on intelligent IoT data processing for smart city," *Comput. Commun.*, vol. 155, pp. 40–47, Apr. 2020.

[20] Y. Xiao, X. Tian, and M. Xiao, "Tourism traffic demand prediction using Google Trends based on EEMD-DBN," *Engineering*, vol. 12, no. 3, pp. 194–215, 2020.

[21] B. Sun, T. Sun, Y. Zhang, and P. Jiao, "Urban traffic flow online prediction based on multi-component attention mechanism," *IET Intell. Transp. Syst.*, vol. 14, no. 10, pp. 1249–1258, Oct. 2020.

[22] X. Shi, H. Qi, Y. Shen, G. Wu, and B. Yin, "A spatial–temporal attention approach for traffic prediction," *IEEE Trans. Intell. Transp. Syst.*, vol. 22, no. 8, pp. 4909–4918, Aug. 2021.

[23] B. Du, X. Hu, L. Sun, J. Liu, Y. Qiao, and W. Lv, "Traffic demand prediction based on dynamic transition convolutional neural network," *IEEE Trans. Intell. Transp. Syst.*, vol. 22, no. 2, pp. 1237–1247, Feb. 2021.

[24] C. Chen, Z. Liu, S. Wan, J. Luan, and Q. Pei, "Traffic flow prediction based on deep learning in Internet of Vehicles," *IEEE Trans. Intell. Transp. Syst.*, vol. 22, no. 6, pp. 3776–3789, Jun. 2021.

[25] A. A. Ceder, "Urban mobility and public transport: Future perspectives and review," *Int. J. Urban Sci.*, vol. 25, no. 4, pp. 455–479, Jul. 2020.

[26] J. Parmar, P. Das, and S. M. Dave, "Study on demand and characteristics of parking system in urban areas: A review," *J. Traffic Transp. Eng.*, vol. 7, no. 1, pp. 111–124, Feb. 2020.

[27] F. Namdarpour, M. Mesbah, A. H. Gandomi, and B. Assemi, "Using genetic programming on GPS trajectories for travel mode detection," *IET Intell. Transp. Syst.*, vol. 16, no. 1, pp. 99–113, Nov. 2021.

[28] M. Mishra, B. Patnaik, R. C. Bansal, R. Naidoo, B. Naik, and J. Nayak, "DTCDWT-SMOTE-XGBoost-Based islanding detection for distributed generation systems: An approach of class-imbalanced issue," *IEEE Syst. J.*, vol. 16, no. 2, pp. 2008–2019, Jun. 2022.

[29] X. Zhu, J. Chu, K. Wang, S. Wu, W. Yan, and K. Chiam, "Prediction of rockhead using a hybrid N-XGBoost machine learning framework," *J. Rock Mech. Geotechnical Eng.*, vol. 13, no. 6, pp. 1231–1245, Dec. 2021.

[30] K. Budholiya, S. K. Shrivastava, and V. Sharma, "An optimized XGBoost based diagnostic system for effective prediction of heart disease," *J. King Saud Univ. Comput. Inf. Sci.*, vol. 34, no. 7, pp. 4514–4523, Jul. 2022.

[31] Y. Kang, S. Shon, and K. Yee, "Local non-intrusive reduced order modeling based on soft clustering and classification algorithm," *Int. J. for Numer. Methods Eng.*, vol. 123, no. 10, pp. 2237–2261, May 2022.

[32] M. A. Imron and B. Prasetyo, "Improving algorithm accuracy K-Nearest neighbor using Z-score normalization and particle swarm optimization to predict customer churn," *JNL. Soft. Comput. Explor.*, vol. 1, no. 1, pp. 56–62, Sep. 2020.

[33] X. Qin, J. Li, W. Hu, and J. Yang, "Machine learning K-means clustering algorithm for interpolative separable density fitting to accelerate hybrid functional calculations with numerical atomic orbitals," *J. Phys. Chem. A*, vol. 124, no. 48, pp. 10066–10074, Dec. 2020.

[34] S. Neelakandan, M. A. Berlin, S. Tripathi, V. B. Devi, I. Bhardwaj, and N. Arulkumar, "IoT-based traffic prediction and traffic signal control system for smart city," *Soft Comput.*, vol. 25, no. 18, pp. 12241–12248, May 2021.

[35] L. Zheng, H. Huang, C. Zhu, and K. Zhang, "A tensor-based K-nearest neighbors method for traffic speed prediction under data missing," *Transportmetrica B, Transp. Dyn.*, vol. 8, no. 1, pp. 182–199, Feb. 2020.

[36] L. Li, H. Zhang, X. Ren, and J. Zhang, "A novel recursive learning identification scheme for Box–Jenkins model based on error data," *Appl. Math. Model.*, vol. 90, pp. 200–216, Feb. 2021.

[37] Y. Bai, M. Tian, M.-L. Tang, and W.-Y. Lee, "Variable selection for ultra-high dimensional quantile regression with missing data and measurement error," *Stat. Methods Med. Res.*, vol. 30, no. 1, pp. 129–150, Jan. 2021.

[38] Z. Tian, "Approach for short-term traffic flow prediction based on empirical mode decomposition and combination model fusion," *IEEE Trans. Intell. Transp. Syst.*, vol. 22, no. 9, pp. 5566–5576, Sep. 2021.

[39] Y. Yu, Y. Zhang, S. Qian, S. Wang, Y. Hu, and B. Yin, "A low rank dynamic mode decomposition model for short-term traffic flow prediction," *IEEE Trans. Intell. Transp. Syst.*, vol. 22, no. 10, pp. 6547–6560, Oct. 2021.

[40] X. Wang, M. Cheng, J. Eaton, C.-J. Hsieh, S. F. Wu, and U. Nvidia, "Fake node attacks on graph convolutional networks," *J. Comput. Cognit. Eng.*, vol. 1 no. 4, pp. 73–165, Oct. 2022.

[41] J. Li, J. Chen, B. Sheng, P. Li, P. Yang, D. D. Feng, and J. Qi, "Automatic detection and classification system of domestic waste via multimodel cascaded convolutional neural network," *IEEE Trans. Ind. Informat.*, vol. 18, no. 1, pp. 163–173, Jan. 2022.

[42] M. Tripathi, "Analysis of convolutional neural network based image classification techniques," *J. Innov. Image Process.*, vol. 3, no. 2, pp. 100–117, Jun. 2021.

[43] B. Liu and Y. Liang, "Optimal function approximation with ReLU neural networks," *Neurocomputing*, vol. 435, pp. 216–227, May 2021.

[44] X. Liu and X. Di, "TanhExp: A smooth activation function with high convergence speed for lightweight neural networks," *IET Comput. Vis.*, vol. 15, no. 2, pp. 136–150, Mar. 2021.

[45] J. Zhang, X. Zhang, J. Wu, and C. Xiao, "Dyeing recipe prediction of cotton fabric based on hyperspectral colour measurement and an improved recurrent neural network," *Coloration Technol.*, vol. 137, no. 2, pp. 166–180, Jan. 2021.

[46] A. K. Das, A. Al Asif, A. Paul, and M. N. Hossain, "Bangla hate speech detection on social media using attention-based recurrent neural network," *J. Intell. Syst.*, vol. 30, no. 1, pp. 578–591, Apr. 2021.
[47] M.-H. Guo, T.-X. Xu, J.-J. Liu, Z.-N. Liu, P.-T. Jiang, T.-J. Mu, S.-H. Zhang, R. R. Martin, M.-M. Cheng, and S.-M. Hu, "Attention mechanisms in computer vision: A survey," *Comput. Vis. Media*, vol. 8, pp. 331–368, Mar. 2022.
[48] H. Zhang, G. Peng, Z. Wu, J. Gong, D. Xu, and H. Shi, "MAM: A multipath attention mechanism for image recognition," *IET Image Process.*, vol. 16, no. 3, pp. 691–702, Feb. 2022.
[49] S. Zhang, Y. Guo, P. Zhao, C. Zheng, and X. Chen, "A graph-based temporal attention framework for multi-sensor traffic flow forecasting," *IEEE Trans. Intell. Transp. Syst.*, vol. 23, no. 7, pp. 7743–7758, Jul. 2022.
[50] B. Fernandes, F. Silva, H. Alaiz-Moreton, P. Novais, J. Neves, and C. Analide, "Long short-term memory networks for traffic flow forecasting: Exploring input variables, time frames and multi-step approaches," *Informatica*, vol. 31, no. 4, pp. 723–749, Jan. 2020.
[51] H. Yang, C. Liu, M. Zhu, X. Ban, and Y. Wang, "How fast you will drive? Predicting speed of customized paths by deep neural network," *IEEE Trans. Intell. Transp. Syst.*, vol. 23, no. 3, pp. 2045–2055, Mar. 2022.
[52] D. Tang, S. Zhang, J. Chen, and X. Wang, "The detection of low-rate DoS attacks using the SADBSCAN algorithm," *Inf. Sci.*, vol. 565, pp. 229–247, Jul. 2021.
[53] B. Turkoglu and E. Kaya, "Training multi-layer perceptron with artificial algae algorithm," *Eng. Sci. Technol., Int. J.*, vol. 23, no. 6, pp. 1342–1350, Dec. 2020.
[54] S. Cheng, F. Lu, and P. Peng, "Short-term traffic forecasting by mining the non-stationarity of spatiotemporal patterns," *IEEE Trans. Intell. Transp. Syst.*, vol. 22, no. 10, pp. 6365–6383, Oct. 2021.
[55] C. Yang, S. Geng, I. Walker, D. T. Branson, J. Liu, J. S. Dai, and R. Kang, "Geometric constraint-based modeling and analysis of a novel continuum robot with shape memory alloy initiated variable stiffness," *Int. J. Robot. Res.*, vol. 39, no. 14, pp. 1620–1634, Apr. 2020.
[56] B. Charbuty and A. Abdulazeez, "Classification based on decision tree algorithm for machine learning," *J. Appl. Sci. Technol. Trends*, vol. 2, no. 1, pp. 20–28, Mar. 2021.
[57] Y. Pan, Y. Wang, P. Zhou, Y. Yan, and D. Guo, "Activation functions selection for BP neural network model of ground surface roughness," *J. Intell. Manuf.*, vol. 31, no. 8, pp. 1825–1836, Dec. 2020.
[58] B. Liu, X. Tang, J. Cheng, and P. Shi, "Traffic flow combination forecasting method based on improved LSTM and ARIMA," *Int. J. Embedded Syst.*, vol. 12, no. 1, p. 22, 2020.
[59] Q. Tao, Z. Li, J. Xu, S. Lin, B. De Schutter, and J. A. K. Suykens, "Short-term traffic flow prediction based on the efficient hinging hyperplanes neural network," *IEEE Trans. Intell. Transp. Syst.*, vol. 23, no. 9, pp. 15616–15628, Sep. 2022.
[60] A. Ali, Y. Zhu, and M. Zakarya, "Exploiting dynamic spatio-temporal correlations for citywide traffic flow prediction using attention based neural networks," *Inf. Sci.*, vol. 577, pp. 852–870, Oct. 2021.

JIAN CUI received the Ph.D. degree in engineering from Chang'an University. She is currently a Postdoctoral Researcher in mobile station with Chang'an University. She is mainly engaged in the scientific research work of transportation tool application engineering, transportation planning, and management. She has published nine academic papers and a utility model patent, including seven SCI and EI journals, two core journals, participated in international academic conferences for many times, and participated in the completion of three scientific research projects.

JIANYOU ZHAO received the Ph.D. degree in engineering from Chang'an University. He is currently a Professor and a Doctoral Supervisor with Chang'an University, where he is also the Director of the Development Research Center. He is also the Deputy Director of the Development Planning Department, Chang'an University, the Deputy Director of Comprehensive Reform Office, and the Deputy Director of the Transportation System Engineering Institute. He is mainly engaged in teaching and scientific research in the fields of transportation tool application engineering, transportation planning and management, transportation information and control engineering, and logistics engineering and management. He has published more than 100 papers, including more than 60 papers included in SCI and EI and have presided over/undertaken more than ten national and provincial scientific research projects in the past five years.